Published in final edited form as:
Cell. 2006 March 10; 124(5): 997–1009. doi:10.1016/j.cell.2005.12.038.

Ligands for clathrin-mediated endocytosis are differentially sorted into distinct populations of early endosomes

Melike Lakadamyali[*], **Michael J. Rust**[*], and **Xiaowei Zhuang**[†]
Department of Chemistry and Chemical Biology, Department of Physics, Howard Hughes Medical Institute, Harvard University, Cambridge, MA 02138

Abstract

Cells rely on the correct sorting of endocytic ligands and receptors for proper function. Early endosomes have been considered as the initial sorting station where cargos for degradation separate from those for recycling. Using live-cell imaging to monitor individual endosomes and ligand particles in real time, we have discovered a sorting mechanism that takes place prior to early endosome entry. We show that early endosomes are in fact comprised of two distinct populations: a dynamic population that is highly mobile on microtubules and matures rapidly towards late endosomes, and a static population that matures much more slowly. Several cargos destined for degradation are preferentially targeted to the dynamic endosomes; whereas the recycling ligand transferrin is non-selectively delivered to all early endosomes and effectively enriched in the larger, static population. This pre-early endosome sorting process begins at clathrin-coated vesicles, depends on microtubule-dependent motility, and appears to involve endocytic adaptors.

Introduction

Proper sorting of proteins and lipids is essential for many cellular activities. Internalized nutrients must be targeted to different organelles for processing and newly synthesized proteins are directed to specific cellular locations for function. A primary function of the endocytic system is to sort internalized ligands and receptors to different destinations (Trowbridge et al., 1993; Mellman, 1996; Mellman and Warren, 2000; Gruenberg, 2001). For example, transferrin, low-density lipoprotein (LDL) receptors, and certain G-protein coupled receptors (GPCR) are recycled back to the plasma membrane (Anderson et al., 1982; Dautry-Varsat et al., 1982; Hopkins and Trowbridge, 1983; Marchese et al., 2003), whereas LDL, epidermal growth factor (EGF), asialoglycoproteins and α-2-macroglobulin are transported to late endosomes and lysosomes for degradation (Carpenter and Cohen, 1979; van Leuven et al., 1980; Wall et al., 1980; Goldstein et al., 1985). Pathogens such as viruses can also exploit endocytic sorting for infection (Pelkmans and Helenius, 2003).

Early endosomes, also referred to as the sorting endosomes, have traditionally been considered as the initial sorting stations, where cargos destined for recycling begin to separate from those bound for degradation (Yamashiro and Maxfield, 1987; Mellman, 1996; Gruenberg, 2001). Transferrin, LDL, and EGF are all believed to first enter a common pool of early endosomes where sorting takes place (Dickson et al., 1983; Dunn et al., 1989; Ghosh et al., 1994). Sorting in the early endosome could result from a geometric constraint in which the membrane-bound

†To whom correspondence should be addressed, E-mail: zhuang@chemistry.harvard.edu. Tel: (617)-496-9558.
*These authors contributed equally to this work.

Additional experimental procedures on cell culture, transfection, RNA interference, immunofluorescence and image analysis are included in Supplemental Material.

components are primarily recycled back to the cell surface, whereas cargos in the fluid phase are more likely to be delivered to late endosomes (Dunn et al., 1989; Mayor et al., 1993; Mellman and Warren, 2000). Lipid composition has also been proposed to play a role in sorting (Mukherjee et al., 1999; Watanabe et al., 1999). In addition, specific sorting signals have been identified on the receptors (Bonifacino and Traub, 2003; Hicke and Dunn, 2003; Marchese et al., 2003; Tanowitz and von Zastrow, 2003; Gruenberg and Stenmark, 2004).

While research efforts have mainly focused on understanding the sorting occurring in early endosomes, a fundamental question remains open as to whether the sorting of endocytic cargos between recycling and degradation pathways may begin even before entering early endosomes. Recently, it has been found that different endocytic receptors require different adaptor proteins for endocytosis (Schmid, 1997; Traub, 2003; Robinson, 2004; Sorkin, 2004). However, the significance of the diversity of adaptor proteins and how these adaptors might direct endocytic sorting remains unclear.

As the endocytic system is comprised of a highly dynamic network of vesicles and endosomes, monitoring the evolution of this network in real-time is crucial for a better understanding of intracellular trafficking. In this work, we observed the trafficking of endocytic ligands by real-time tracking of the interactions between individual cargo particles and endosomes in live cells. We show that early endosomes are not made of a uniform pool of endocytic compartments non-discriminatively accepting all internalized cargos, but instead are comprised of two populations with distinct mobility and maturation kinetics. Surprisingly, ligands such as transferrin, LDL, EGF, and influenza virus, which all enter cells primarily via clathrin-mediated endocytosis, are differentially trafficked into these two populations: those ligands destined for degradation are preferentially targeted to the small population of dynamic, rapidly maturing early endosomes, whereas the recycling ligand transferrin is non-selectively targeted to all early endosomes and effectively enriched in the larger population of static, slowly maturing early endosomes. This pre-early endosome sorting begins at the plasma membrane and depends on the composition and motility of endocytic vesicles.

Results

Early endosomes are comprised of two distinct populations with different maturation kinetics and mobility

Rab GTPases are specifically localized to different intracellular organelles (Zerial and McBride, 2001; Pfeffer and Aivazian, 2004). For example, Rab5 and Rab7 primarily associate with early and late endosomes, respectively, and Rab11 is a recycling endosome marker, though small amounts of Rab11 were also found in early endosomes and Golgi (Chavrier et al., 1990; Ullrich et al., 1996; Sonnichsen et al., 2000; Barbero et al., 2002). In order to visualize early and late endosomes, we co-expressed Rab5 and Rab7, fused to cyan and yellow fluorescent proteins (ECFP and EYFP) respectively, in BS-C-1 cells. ECFP-Rab5 shows discrete spots primarily distributed in the cell periphery; EYFP-Rab7 spots are more common in the perinuclear region (Movie S1). While most of the Rab5-positive endosomes show only the Rab5 signal, a small fraction (~14%) contains partially overlapping domains of Rab5 and Rab7. We interpret the former as early endosomes and the latter as transient intermediates, which are maturing toward late endosomes (Stoorvogel et al., 1991; Rink et al., 2005; Vonderheit and Helenius, 2005). Indeed, the Rab5-only endosomes show 80% colocalization with early endosomal antigen 1 (EEA1) (Figure 1A), but only 10% colocalization with a late endosome marker, the cation-independent mannose phosphate receptor (CI-MPR) (Figure 1B). In contrast, 57% of the endosomes that contain both Rab5 and Rab7 overlap with CI-MPR (Figure 1B). Substantial over-expression of Rab5 was previously shown to cause pronounced enlargement of early endosomes and their redistribution to the perinuclear region (Nielsen et al., 1999). In our experiments, ECFP-Rab5 was expressed at sufficiently low levels such that

the enlargement and redistribution of endosomes were not observed. The expression of ECFP-Rab5 and EYFP-Rab7 also did not affect the internalization and post-endocytic trafficking kinetics of endocytic ligands (Figures S1, S2).

Next, we tracked early endosomes that initially carry Rab5 and observed the change of their Rab content in real time (Figures 1C, D and Movies S2, S3). Surprisingly, we observed two distinct populations of early endosomes: about 35% of Rab5-positive endosomes either mature rapidly by accumulating Rab7 with a time constant of 30 s or already carry Rab7 at the beginning of our observation; the remaining 65% mature on a much slower time scale, not acquiring Rab7 even after 100 s (Figure 1E). The accumulation of Rab7 mostly occurs gradually (Figure 1D). The maturation kinetics are identical between cells maintained at 37° C and cells that have just experienced a temperature jump from 0°C to 37°C (Figure S3).

The maturation rate of early endosomes is highly correlated with their mobility along microtubules (Figure 1F). The rapidly maturing population shows significantly higher mobility and exhibits directed movement, demonstrated by a mean-square-displacement analysis of the endosome trajectories (Figure S4). In contrast, the slowly maturing population is much less mobile. The mobility of the rapidly maturing population is reduced to the level of the slowly maturing endosomes by treatment with the microtubule-disrupting drug nocodazole (Figure 1F), indicating that the rapidly maturing population is actively transported on microtubules whereas the slowly maturing population is not. Some of the slowly maturing endosomes eventually acquire Rab7 before significant photobleaching begins to interfere with imaging. Shortly before Rab7 accumulation, the mobility of these endosomes typically increases to a level similar to that of the rapidly maturing population (not shown), suggesting that the two observed populations may represent two different stages in the life cycle of early endosomes.

The existence of two populations of early endosomes naturally raises the question of whether these populations are functionally distinct. To address this, we used real-time, three-color imaging to track individual cargo particles as they entered Rab-labeled endosomes.

Preferential targeting of LDL, EGF and influenza to the dynamic population of early endosomes

We first tested the trafficking of cargos destined for degradation, including LDL, EGF, and influenza virus. LDL delivers cholesterol into cells by clathrin-mediated endocytosis (Anderson et al., 1977). In order to determine whether the two populations of early endosomes are equally efficient in accepting LDL, we imaged the uptake of fluorescently labeled LDL in live cells. Remarkably, the great majority of internalized LDL is directly targeted to the dynamic, rapidly maturing endosomes (Figure 2A and Movie S4). Even though this population represents only 35% of all early endosomes, 80% of LDL particles are directed to these structures (Figure 2B). In particular, 53% of LDL particles are delivered to endosomes that already contain both Rab5 and Rab7, indicating that LDL is indeed preferentially targeted to this population instead of stimulating the acquisition of Rab7. The delivery of LDL to dynamic endosomes often occurs soon after the LDL-carrying vesicle undergoes microtubule-dependent transport (Figure 2C).

EGF primarily enters cells via clathrin-mediated endocytosis when added at low concentrations (Carpenter and Cohen, 1979). At high concentrations, some EGF molecules are diverted to other pathways (Jiang and Sorkin, 2003; Chen and De Camilli, 2005; Sigismund et al., 2005). At the concentration used here, we found that EGF clusters into discrete structures on the cell surface and nearly all of these clusters colocalize with clathrin-coated pits before entry (not shown). Much like LDL, upon internalization, EGF is preferentially targeted directly to the dynamic, rapidly maturing population of early endosomes (86%) with only a small fraction (14%) joining the static, slowly maturing endosomes.

Influenza virus enters cells by multiple endocytic mechanisms (Matlin et al., 1981; Sieczkarski and Whittaker, 2002) and subsequent fusion with late endosomes to release its genetic material (Yishimura and Ohnishi, 1984). We have previously shown that influenza virus primarily enters cells via clathrin-mediated endocytosis (65%), with a small fraction (35%) entering via a clathrin- and caveolin-independent pathway (Rust et al., 2004). To observe the trafficking of influenza, we added DiD-labeled virus particles to cells *in situ* while imaging. Like LDL, the virus particles are preferentially directed to the dynamic population of early endosomes (Figures 3A, B and Movie S5). Again, the majority of virus particles join endosomes after the onset of microtubule-dependent transport (Figures 3C, D). This is also consistent with our previous observation that the virus particles experience their initial acidification to pH6 (early endosome pH) after the onset of microtubule-dependent transport (Lakadamyali et al., 2003). Viral fusion events are identified by fluorescence dequenching due to spreading of DiD into the larger endosomal membrane (Figure 3A and Movie S5) (Lakadamyali et al., 2003). Interestingly, the majority of fusion events (72%) occur in maturing endosomes when both Rab5 and Rab7 are present (Figure 3A).

Non-selective trafficking of transferrin to all early endosomes

Transferrin delivers iron to cells by clathrin-mediated endocytosis (Hopkins and Trowbridge, 1983). Internalized transferrin was previously believed to initially follow the same path taken by LDL, entering a common set of early endosomes before being recycled to the plasma membrane (Dunn et al., 1989; Ghosh et al., 1994). Surprisingly, our real-time tracking of transferrin indicates that the initial trafficking of transferrin is drastically different from that of LDL. Transferrin shows more than 90% colocalization with all Rab5-positive endosomes after uptake (Figure 4A). In single-particle tracking experiments, transferrin-carrying vesicles, which initially exhibit no detectable Rab5 signal, are non-discriminately delivered to both populations of early endosomes (Figures 4B,C). Since the static, slowly maturing endosomes constitute a larger population than the dynamic, rapidly maturing ones, the effective result is that most of the transferrin molecules are delivered to the static population. This difference in transferrin and LDL trafficking is quantitatively consistent with the global distributions of these ligands obtained in cells expressing (or not expressing) fluorescent Rab proteins by using Rab5 and Rab7 (or EEA1 and CI-MPR) as the endosome markers (Figure S5). The results are also independent of whether or not a low-temperature ligand-binding step was employed prior to uptake.

In cells expressing EYFP-Rab11, a recycling endosome marker, transferrin molecules were observed to join Rab11-positive endosomes (Figure 4D, Movie S6), indicating that they were indeed delivered to the recycling pathway. Drugs interfering with recycling, such as wortmannin and neomycin, substantially reduce the percentage of transferrin spots colocalizing with Rab11 (not shown). Besides going through the recycling endosomes, transferrin can also take a direct recycling pathway back to the cell surface (Sheff et al., 1999; Sheff et al., 2002). Typically within minutes (96 +/− 44 sec on average) of association with Rab11, the transferrin spot forms tubular structures and breaks up into optically resolvable smaller vesicles (Figure 4D, Movie S6), indicating tubular segments of endosomes pinching off to recycle transferrin back to the cell surface (Sonnichsen et al., 2000; Rink et al., 2005). Consistent with this notion, such tubulation behavior was not observed for ligands destined to degradation, such as LDL or EGF. The tubulation of transferrin was observed from both static and dynamic early endosomes, including those containing both Rab5 and Rab7, suggesting that transferrin can be recycled from both endosome populations.

Differential sorting into distinct early endosome populations is pH-independent

The acidity of the early endosome (~pH 6) is important for its ability to sort cargos between degradation and recycling pathways (Mellman et al., 1986). To observe the initial entry of

cargo into an acidic endosome, we tracked influenza virus particles labeled with pH-sensitive dyes (Lakadamyali et al., 2003). The initial acidification step coincides with viral entry into a Rab5-positive endosome (Figures 3E,F), indicating that prior to the association with Rab5, the cargo did not join any acidic endosome. In addition, treatment with ammonium chloride to raise endosome pH did not affect the differential sorting of LDL and transferrin into the dynamic and static populations of early endosomes (Figure 5A), indicating that this pre-early endosome sorting is pH-independent, unlike the sorting process inside the early endosomes.

Differential sorting into distinct early endosome populations requires microtubules

An important difference between the two populations of early endosomes is that the rapidly maturing endosomes are highly mobile along microtubules while the slowly maturing ones are largely stationary. This, together with the observation that LDL and influenza mostly join early endosomes after the onset of microtubule-dependent transport, suggests that microtubules may play an important role in preferentially targeting these cargos to the dynamic, rapidly maturing endosome population. This is strongly supported by the observation that treatment with nocodazole to disrupt microtubules resulted in LDL and influenza non-selectively joining all early endosomes, just like transferrin (Figure 5B). We infer from these results that endocytic vesicles with microtubule-dependent motility will be preferentially delivered to dynamic, rapidly maturing endosomes which are also moving on microtubules, whereas vesicles lacking microtubule-dependent motility will non-selectively join all early endosomes.

The pre-early endosome sorting begins at the plasma membrane

The endocytic cargos studied in this work are all primarily internalized via clathrin-mediated endocytosis. The clathrin coat on nascent endocytic vesicles must be shed before the vesicle can fuse with endosomes (Bonifacino and Lippincott-Schwartz, 2003). To measure the delay between clathrin uncoating and cargo delivery to Rab5-positive endosomes, we imaged influenza uptake in cells co-expressing ECFP-Rab5 and EYFP-clathrin. The brief delay detected (16 sec +/− 7 sec) is unlikely to be sufficient for the uncoated endocytic vesicle to be processed through an undetected sorting compartment before joining an early endosome. Therefore, it is likely that cargo sorting already occurs at the clathrin-coated vesicle level, and that LDL, EGF and influenza may be sorted to a subpopulation of coated vesicles, which are directly targeted to the dynamic early endosomes immediately after their detachment from the plasma membrane.

Consistent with this hypothesis, only a small fraction of clathrin-coated pits (CCPs) were observed to efficiently take up LDL whereas most CCPs readily take up transferrin (Figures 6A–C). The fraction of CCPs loaded with LDL initially increases with LDL concentration, but saturates near 15% at 37°C (Figure 6C). These results suggest that only a small subset of CCPs can efficiently accept LDL. While it is formally possible that the saturation behavior is caused by saturating all LDL receptors (LDLRs), we consider this less likely for the following reasons: (1) The number of LDL particles bound to the cell continues to increase linearly with LDL concentration in the saturation region (not shown); (2) Nonspecific binding of LDL was not detected even at a concentration 8 times larger than the maximum concentration used here (Anderson et al., 1977); (3) Up-regulating LDLR expression by overnight-incubation of cells with lipoprotein-deficient serum did not increase the fraction of CCPs occupied by LDL (Figure 6C). Using longer LDL incubation times at 37°C did not change the saturation level, indicating that a dynamic equilibrium was reached. Similar results were also obtained when LDL binding was performed at 4°C for 10 min (Figure 6B). However, a much higher fraction of CCPs (~50%) were loaded with LDL when a 2 hr binding step at 4°C was used, consistent with previous observations (Anderson et al., 1977), indicating that most pits may eventually acquire the ability to recruit LDL given sufficient time under a condition where the formation of new pits is inhibited. However, the observation that the fraction of CCPs occupied by LDL saturates

at 15% at 37°C, in spite of the increasing density of LDL bound to the cell surface, suggests that a small subset of CCPs accepts LDL much more readily than the remaining ones. Similarly, only a small fraction of CCPs were loaded with EGF at 37°C, no matter how high an EGF concentration was used (Figure 6D).

We also imaged the Disabled-2 (Dab2) protein, a specific endocytic adaptor for LDLR (Traub, 2003), together with LDL and clathrin, after incubating the cells with various concentrations of LDL at 37°C. CCPs show significant colocalization with Dab2 and the quantitative extent of colocalization is cell-type dependent (Figure S6A) (Morris and Cooper, 2001). In BSC-1 cells, roughly 30% of CCPs contain detectable amount of Dab2. The fraction of Dab2-positive CCPs containing LDL saturates at 25% at 37°C. This fraction is 2-fold higher than that for Dab2-negative CCPs (Figure 6E). A quantitatively similar trend was also found in HeLa cells (Figure S6B), which exhibit a substantially higher Dab2-CCP colocalization (Figure S6A). These results indicate that a Dab2-enriched CCP is more likely to associate with LDL than a Dab2-deficient CCP.

The role of endocytic adaptor proteins in the pre-early endosome sorting

Although LDL, EGF, influenza and transferrin are all internalized via clathrin-mediated endocytosis, the requirements for adaptor proteins are different. Using siRNA against the μ2 subunit of the AP-2 adaptor, we show that the uptake of transferrin is blocked by the AP-2 knockdown (Figures S7A, B), but the internalization rate and extent of uptake for LDL and EGF are not affected (Figures S7C, D), consistent with previous findings (Nesterov et al., 1999; Conner and Schmid, 2003; Hinrichsen et al., 2003; Motley et al., 2003). The AP-2-independent uptake of EGF may be promoted by a low-temperature binding step (Huang et al., 2004). Moreover, the internalization kinetics of influenza and the fraction of influenza viruses entering via clathrin-mediated endocytosis are also unaffected by AP-2 knockdown (Figure S7E), indicating that the clathrin-mediated endocytosis of influenza is independent of AP-2. These results suggest an interesting correlation between adaptor protein requirement and the observed pre-early endosomal sorting behavior: the AP-2-independent ligands, LDL, EGF, and influenza, are all preferentially targeted to the dynamic, rapidly maturing early endosomes, whereas the AP-2-dependent ligand transferrin is nonselective delivered to all early endosomes.

To further test the involvement of endocytic adaptors in sorting, we determined the overall distribution of rapidly and slowly maturing endosomes in the AP-2 knockdown cells. Remarkably, the balance between the two populations is dramatically shifted. In contrast to the untreated cells where only a minority (35%) of early endosomes matures rapidly, in the AP-2 knockdown cells, most of early endosomes (78%) belong to the dynamic, rapidly maturing population (Figure 5C). This shift is due to a large reduction in the total density of slowly maturing endosomes (by 8 fold), while the density of rapidly maturing endosomes remains unchanged (within 10%). Considering that the fusion of endocytic vesicles is a major contribution to the biogenesis of the early endosomes, this observation links the dynamic early endosome population to the AP-2 independent endocytic vesicles and suggests that endocytic adaptor proteins play an important role in sorting endocytic vesicles to the different populations of early endosomes.

Discussion

Receptor-mediated endocytosis is a major mechanism by which cells take up nutrients and signaling molecules and down-regulate receptors on the cell surface. Due to its highly dynamic nature, how the endocytic network evolves over time remains incompletely understood. Recent advances in fluorescence microscopy allow the dynamics of microscopic cellular structures to be imaged in live cells. This capability can provide unique information critical for

understanding the time-dependent behavior of the endocytic network. Indeed, real-time imaging of endocytic structures, such as the clathrin-coated vesicles, has substantially improved our understanding of their biogenesis (Gaidarov et al., 1999; Merrifield et al., 2002; Ehrlich et al., 2004; Merrifield et al., 2005; Rink et al., 2005). Tracking individual cargo particles in live cells has elucidated specific uptake mechanisms (Pelkmans et al., 2004; Rust et al., 2004; Vonderheit and Helenius, 2005).

In this study, using live-cell imaging to track the interaction between various endocytic ligands and endosomes at the single-particle level, we provide direct evidence that cargos destined for the degradation and recycling pathways are differentially sorted into two distinct populations of early endosomes, despite all being internalized via clathrin-mediated endocytosis. The mechanism underlying this pre-early endosome sorting process is discussed below.

The early endosomes consist of two populations with distinct maturation kinetics and mobility

The endocytic pathway is primarily comprised of three types of endosomes: the early, recycling and late endosomes. Endocytosed cargos were believed to first enter a common pool of early endosomes. Subsequently, receptors and ligands destined for recycling are delivered back to the cell surface; cargos bound for degradation are sorted to late endosomes and lysosomes (Trowbridge et al., 1993; Mellman, 1996; Mellman and Warren, 2000; Gruenberg, 2001).

Using fluorescent Rab GTPases to mark endosomes and tracking them in live cells, we have discovered that early endosomes are not a homogeneous pool of organelles, but in fact consist of two distinct populations (Figure 1). The first population is highly mobile on microtubules and matures rapidly toward late endosomes, as indicated by the accumulation of Rab7. The second population is largely static, shows little microtubule-dependent motility, and matures much more slowly.

Cargos destined for the degradation pathway, once having joined a Rab5-positive early endosome, remain associated with that endosome while Rab7 accumulates (Figure 2, Figure 3). These Rab5- and Rab7 co-positive endosomes eventually lose their Rab5 content, either by gradual dissociation of Rab5 or by fission of the Rab5-positive domain (Rink et al., 2005;Vonderheit and Helenius, 2005). The choice between the two appears to be cargo-dependent (M.J.R., M.L., X.Z., unpublished).

It is interesting to note that early endocytic vesicles with special functions have been reported previously (Bomsel et al., 1989; Hughson and Hopkins, 1990; Parton et al., 1992; Mundigl et al., 1993; Wei et al., 1998): certain apical endosomes in epithelial cells are thought to perform cell-type specific functions but do not take up “house-keeping” receptors and ligands; specialized endosomes also exist in neurons to recycle synaptic vesicles. These specialized endosomes are, however, unlikely to be related to the two early endosome populations reported here, both of which colocalize with conventional early endosome markers and receive “house-keeping” endocytic ligands. These populations are functionally distinct in that different ligands are differentially sorted to the two populations, as we discuss below.

Cargo destined for degradation and recycling are differentially sorted into the two populations of early endosomes

To date, early endosomes have been viewed as the initial sorting station; cargos for recycling and degradation were thought to first enter a common pool of early endosomes before sorting begins. By tracking endocytic cargo in live cells, we provide direct evidence for a pre-early endosome sorting process: while the recycling ligand transferrin enters both populations of early endosomes indiscriminately, LDL and EGF, which are bound for degradation, are almost

predominantly targeted to the population of dynamic, rapidly maturing endosomes (Figure 2, Figure 4, and Figure S5). Influenza virus is also preferentially targeted to this dynamic population (Figure 3). It is worth noting that this pre-early endosome sorting would have been difficult to observe without real-time single-particle tracking. Since transferrin non-selectively enters all early endosomes, the ones containing LDL will also contain transferrin when both ligands are present (Figure S5E), just as previously observed (Dunn et al., 1989;Ghosh et al., 1994). A quantitative analysis of the global distributions of LDL and transferrin indeed supports the pre-early endosome sorting picture (Figure S5).

In addition, we found that transferrin can be recycled from both populations of early endosomes. Taken together, these observations indicate that there are at least two stages of sorting between the recycling and degradation pathways. In addition to the well known sorting process that occurs in the early endosome, an earlier sorting stage occurs even before the cargo enters early endosomes. At this earlier stage, several investigated cargos destined for degradation are predominately targeted to a small population of dynamic, rapidly maturing endosomes, but the recycling cargo transferrin enters all early endosomes non-selectively. Since the static, slowly maturing endosomes substantially outnumber the dynamic ones, transferrin is effectively enriched in the former population.

The origin of pre-early endosome sorting

Several pieces of evidence suggest that the observed differential sorting of endocytic cargos to the two early endosome populations originates at the plasma membrane. First, the entry of cargo into the Rab5-positive endosomes occurs within seconds after the endocytic vesicles shed their clathrin coat, leaving little time for the cargo to be processed by yet another sorting compartment. Second, endocytic cargos experience their initial exposure to an acidic environment as they enter a Rab5-positive endosome (Figures 3E, F), and the observed pre-early endosome sorting is pH-independent (Figure 5A), eliminating the possibility of an undetected acidic sorting endosome. Finally, nearly all CCPs readily accept transferrin (Figure 6), whereas only a small fraction of CCPs take up LDL and EGF at 37°C, no matter how high a LDL or EGF concentration is used (Figure 6, Figure S6), suggesting that a small subset of CCPs more readily accept LDL and EGF than the remaining ones. Notably, a Dab2-enriched CCP is more likely to associate with LDL than a Dab2-deficient CCP (Figure 6E, Figure S6B), suggesting that Dab2 might partially contribute to the observed sorting behavior. This is consistent with the specific interactions identified between Dab2 and the internalization motif of LDLR (Morris and Cooper, 2001; Traub, 2003). However, even among Dab2-positive CCPs, only a small fraction readily take up LDL at 37°C (Figure 6E, Figure S6B), suggesting that important additional sorting factors are involved. Interestingly, another endocytic ligand, β-2AR, was also found to be enriched in coated vesicles containing a cargo-specific adaptor, β-arrestin (Cao et al., 1998).

Adaptor proteins are critical components of clathrin-coated vesicles, playing an important role in cargo recruitment. AP-2 was previously believed to be a universal adaptor for all clathrin-mediated endocytosis. However, it was recently found that, while transferrin requires AP-2 for internalization, the entry of LDL and EGF can proceed without AP-2, presumably by using alternative adaptors (Conner and Schmid, 2003; Hinrichsen et al., 2003; Motley et al., 2003; Huang et al., 2004). Cargo-specific adaptors Dab2, ARH, epsins, HIP1/Hip1R and AP180 have been proposed as possible candidates (Traub, 2003). Our experiments confirm these previous results and further show the clathrin-mediated endocytosis of influenza is also independent of AP-2 (Figure S7). These results suggest a potential correlation between adaptor proteins and pre-early endosome sorting: the cargos not requiring AP-2 for entry are preferentially targeted to the dynamic population of early endosomes, potentially due to the presence of alternative adaptors on the endocytic vesicles. Considering that fusion between endocytic vesicles is a

major contribution to the biogenesis of early endosomes, this hypothesis predicts that depleting AP-2 should significantly increase the relative fraction of endocytic vesicles carrying alternative adaptors, which would be targeted to dynamic early endosomes or fuse with each other to form dynamic endosomes, therefore leading to a change in the balance between the two endosome populations. This is indeed observed: AP-2 knockdown drastically reduces the number of static endosomes while leaving the number of dynamic endosomes unchanged. As a result, the relative population of dynamic, rapidly maturing endosomes is substantially increased (Figure 5C), consistent with the hypothesis that the dynamic population of early endosomes is linked to the AP-2 independent endocytic vesicles.

Finally, effective pre-early endosome sorting depends critically on an intact microtubule cytoskeleton. Disrupting microtubules removes the observed selective trafficking, causing LDL and influenza to be targeted indiscriminately to all early endosomes in a way similar to transferrin (Figure 5B). This is consistent with the observations that endocytic vesicles containing LDL or influenza typically join dynamic early endosomes after the onset of microtubule-dependent movement, and that rapidly maturing endosomes show high mobility on microtubules, whereas the slowly maturing endosomes are largely immobile. Thus the pre-early endosome sorting is determined by microtubule-dependent motility of the endocytic vesicles: the vesicles with the ability to rapidly engage microtubules after detachment from the plasma membrane are more likely to encounter a dynamic, rapidly maturing endosome which is itself moving on microtubules.

Taken together, we propose the following model for the observed pre-early endosome sorting (Figure 7). Early endosomes are comprised of two distinct populations: a dynamic population that is highly mobile on microtubules and matures quickly towards late endosomes, and a static population that matures much more slowly. These populations are functionally different in the uptake of endocytic cargo. Several cargos destined for degradation, including LDL, EGF and influenza virus, are internalized by a subpopulation(s) of clathrin-coated vesicles, which likely contain alternative adaptors in addition to AP-2. These vesicles rapidly engage microtubules and are consequently targeted to the dynamic population of early endosomes, which are also moving on microtubules. The recycling ligand transferrin is indiscriminately recruited to all clathrin-coated vesicles and thus delivered to both populations of early endosomes non-selectively. As a result, transferrin is effectively enriched in the larger, static population of early endosomes. The extent to which the correlation between the final fate of an endocytic ligand (in terms of degradation and recycling) and their pre-early endosome sorting is general and applicable to other ligands remains to be addressed. This model also suggests an intriguing connection between certain endocytic adaptors and microtubule-dependent motility, the plausibility of which is supported by the microtubule-binding activity of several cargo-specific adaptor proteins (Kittel and Komori, 1999;Hussain et al., 2003).

Experimental procedures

Materials

BS-C-1 cells were from ATCC. Purified influenza virus X-31 was from Charles River Laboratories. DiD-, CypHer5-, and Cy3-labeling of the viruses was carried out as previously described (Lakadamyali et al., 2003). Purified LDL was from Biomedical Technologies and labeled with DiD or Cy5. Alexa 647-labeled EGF and transferrin were from Molecular Probes. Antibodies against the clathrin heavy chain (Santa Cruz Biotechnologies), EEA1 (Abcam), CI-MPR (Affinity Bioreagents), α-subunit of AP-2 (Affinity Bioreagents), and Dab2 (Santa Cruz Biotechnologies and Transduction Labs) were used for immunofluorescence. Plasmids encoding ECFP-Rab5, EYFP-Rab5 and EYFP-Rab11 are gifts from M. Zerial. Plasmid encoding EYFP-Rab7 were constructed from ECFP-Rab7, a gift from S. Pfeffer. This plasmid was digested with *Xho*I and *Kpn*I to isolate the gene encoding Rab7. This gene was then inserted

into the pEYFP-C1 vector (Clontech). GFP-clathrin LC*a* was a gift from J. Keen and the EYFP-clathrin LC*a* was previously constructed (Rust et al., 2004). siRNA against the μ2 subunit of AP-2 (AAGUGGAUGCCUUUCGGGUCA) (Motley et al., 2003) was from Dharmacon.

Uptake and trafficking of transferrin, LDL, EGF and influenza

Influenza virus was added to cells *in situ* at 37 °C during image acquisition. Transferrin, LDL and EGF binding were performed at 0°C or 37°C, as specified. Labeled transferrin, LDL, and EGF were added to cells at a concentration of 20 μg/mL, 33 μg/mL, and 0.2 μg/mL, respectively, unless otherwise specified. At 0.2 μg/mL, we found that EGF still primarily enters BS-C-1 cells via clathrin-mediated endocytosis, although previous studies with different cell types have indicated a substantial diversion to a clathrin-independent pathway at a lower concentration (Jiang and Sorkin, 2003; Sigismund et al., 2005), potentially due to a cell type difference. The uptake and endocytic trafficking of these ligands were imaged at 37 °C on a temperature-controlled microscope.

Live-Cell fluorescence imaging

We took three-color fluorescence images of ECFP, EYFP or Cy3, and red fluorescent dyes (DiD, Alexa 647, or CypHer5) by simultaneously exciting fluorophores with a 454 nm argon laser (Melles-Griot), a 532 nm Nd:YAG laser (Crystalaser) and a 633 nm helium-neon laser (Melles-Griot), respectively. The 633 nm excitation was continuous, while the 454nm and 532 nm excitations were alternated at 0.5 Hz. Short- (from ECFP, EYFP or Cy3) and long-wavelength emissions (from DiD, Alexa 647, or CypHer5) were collected by a 1.4 N.A. objective (Olympus), separated by 650 nm long-pass dichroic mirrors (Chroma) and imaged by a CCD camera (CoolSNAP HQ, Roper Scientific). The long wavelength images were acquired at 2 frames per second through a 665 nm long-pass filter. To collect alternating images of ECFP and EYFP (or Cy3), a motorized filter wheel was placed in the short-wavelength path and toggled between a 480/40 nm bandpass filter (for ECFP) and a 585/35 bandpass filter (for EYFP or Cy3) at 0.5 Hz, in synch with the alternating 454 nm and 532 nm excitations.

Supplementary Material

Refer to Web version on PubMed Central for supplementary material.

Acknowledgement

We thank M. Zerial, S. Pfeffer and J. Keen for their generous gifts of the ECFP-Rab5, EYFP-Rab11, ECFP-Rab7 and GFP-LCa plasmids. This work is supported in part by the National Institute of Health (NIGMS), the Searle Scholar Program (Kinship foundation), and the Arnold and Mabel Beckman foundation (to X.Z.). X.Z. is a Howard Hughes Medical Institute Investigator. M.J.R. is a National Science Foundation pre-doctoral fellow.

References

Anderson RGW, Brown MS, Beisiegel U, Goldstein JL. Surface distribution and recycling of the low density lipoprotein receptor as visualized with antireceptor antibodies. J Cell Biol 1982;93:523–531. [PubMed: 6288727]

Anderson RGW, Brown MS, Goldstein JL. Role of the coated endocytic vesicle in the uptake of receptor-bound low density lipoprotein in human fibroblasts. Cell 1977;10:351–364. [PubMed: 191195]

Barbero P, Bittova L, Pfeffer SR. Visualization of Rab9-mediated vesicle transport from endosomes to the trans-Golgi in living cells. J Cell Biol 2002;156:511–518. [PubMed: 11827983]

Bomsel M, Prydz K, Parton RG, Gruenberg J, Simons K. Endocytosis in filter-grown madin-darby canine kidney-cells. J Cell Biol 1989;109:3243–3258. [PubMed: 2689455]

Bonifacino JS, Lippincott-Schwartz J. Coated Proteins: shaping membrane transport. Nat Rev Mol Cell Biol 2003;4:409–414. [PubMed: 12728274]

Bonifacino JS, Traub LM. Signals for sorting of transmembrane proteins to endosomes and lysosomes. Annu Rev Biochem 2003;72:395–447. [PubMed: 12651740]

Cao TT, Mays RW, Zastrow M. Regulated endocytosis of G-protein-coupled receptors by a biochemically and functionally distinct subpopulation of clathrin-coated pits. J Biol Chem 1998;273:24592–24602. [PubMed: 9733754]

Carpenter G, Cohen S. Epidermal growth-factor. Ann Rev Biochem 1979;48:193–216. [PubMed: 382984]

Chavrier P, Parton RG, Hauri HP, Simons K, Zerial M. Localization of low molecular weight GTP binding proteins to exocytic and endocytic compartments. Cell 1990;62:317–329. [PubMed: 2115402]

Chen H, De Camilli P. The association of epsin with ubiquitinated cargo along the endocytic pathway is negatively regulated by its interaction with clathrin. Proc Natl Acad Sci, USA 2005;102:2766–2771. [PubMed: 15701696]

Conner SD, Schmid SL. Differential requirements for AP-2 in clathrin-mediated endocytosis. J Cell Biol 2003;162:773–779. [PubMed: 12952931]

Dautry-Varsat A, Ciechanover A, Lodish H. pH and the recycling of transferrin during receptor-mediated endocytosis. Proc Natl Acad Sci U S A 1982;80:2258–2262. [PubMed: 6300903]

Dickson RB, Hanover JA, Willingham MC, Pastan I. Prelysosomal divergence of transferrin and epidermal growth factor during receptor-mediated endocytosis. Biochem 1983;22:5667–5674. [PubMed: 6317024]

Dunn KW, McGraw TE, Maxfield FR. Iterative fractionation of recycling receptors from lysosomally destined ligands in an early sorting endosome. J Cell Biol 1989;109:3303–3314. [PubMed: 2600137]

Ehrlich M, Boll W, van Oijen AM, Hariharan R, Chandran K, Nibert ML, Kirchhauen T. Endocytosis by random initiation and stabilization of clathrin-coated pits. Cell 2004;118:591–605. [PubMed: 15339664]

Gaidarov I, Francesca S, Warren RA, Keen JH. Spatial control of coated-pit dynamics in living cells. Nat Cell Biol 1999;1:1–7. [PubMed: 10559856]

Ghosh RN, Gelman DL, Maxfield FR. Quantification of low density lipoprotein and transferrin endocytic sorting in HEp2 cells using confocal microscopy. J Cell Sci 1994;107:2177–2189. [PubMed: 7983176]

Goldstein JL, Brown MS, Anderson RGW, Russell DW, Schneider WJ. Receptor-mediated endocytosis: concepts emerging from the LDL receptor system. Ann Rev Cell Biol 1985;1:1–39. [PubMed: 2881559]

Gruenberg J. The endocytic pathway: A mosaic of domains. Nat Rev Mol Cell Biol 2001;2:721–730. [PubMed: 11584299]

Gruenberg J, Stenmark H. The biogenesis of multivesicular endosomes. Nat Rev Mol Cell Biol 2004;5:317–323. [PubMed: 15071556]

Hicke L, Dunn R. Regulation of membrane protein transport by ubiquitin and ubiquitin-binding proteins. Annu Rev Cell Biol 2003;19:141–172.

Hinrichsen L, Harborth J, Andrees L, Weber K, Ungewickell EJ. Effect of clathrin heavy chain- and α-adaptin specific small inhibitory RNAs on endocytic accessory proteins and receptor trafficking in HeLa cells. J Biol Chem 2003;278:45160–45170. [PubMed: 12960147]

Hopkins CR, Trowbridge IS. Internalization and processing of transferrin and the transferrin receptor in human carcinoma A431 cells. J Cell Biol 1983;97:508–521. [PubMed: 6309862]

Huang F, Khvorova A, Marshall W, Sorkin A. Analysis of clathrin-mediated endocytosis of epidermal growth factor receptor by RNA interference. J Biol Chem 2004;279:16657–16661. [PubMed: 14985334]

Hughson EJ, Hopkins CR. Endocytic pathways in polarized caco-2 cells - identification of an endosomal compartment accessible from both apical and basolateral surfaces. J Cell Biol 1990;110:337–348. [PubMed: 2298809]

Hussain NK, Yamabhai M, Bhakar AL, Metzler M, Ferguson SSG, Hayden MR, McPherson PS, Kay BK. A role for epsin N-terminal homology/AP180 N-terminal homology (ENTH/ANTH) domains in tubulin binding. J Biol Chem 2003;278:28823–28830. [PubMed: 12750376]

Jiang X, Sorkin A. Epidermal growth factor receptor internalization through clathrin-coated pits requires CbI RING finger and proline-rich domains but not receptor polyubiquitylation. Traffic 2003;4:529–543. [PubMed: 12839496]

Kittel A, Komori N. Ultrastructural localization of beta-arrestin-1 and -2 in rat lumbar spinal cord. J Com Neuro 1999;412:649–655.

Lakadamyali M, Rust MJ, Babcock HP, Zhuang X. Visualizing infection of individual influenza viruses. Proc Natl Acad Sci, USA 2003;100:9280–9285. [PubMed: 12883000]

Marchese A, Catherine C, Kim Y-M, Benovic JL. The ins and outs of G protein-coupled receptor trafficking. Trends Biochem Sci 2003;28:369–375. [PubMed: 12878004]

Matlin KS, Reggio H, Helenius A, Simons K. Infectious entry pathway of influenza virus in a canine kidney-cell line. J Cell Biol 1981;91:601–613. [PubMed: 7328111]

Mayor S, Presley JF, Maxfield FR. Sorting of membrane components from endosomes and subsequent recycling to the cell serface occurs by a bulk flow process. J Cell Biol 1993;121:1257–1269. [PubMed: 8509447]

Mellman I. Endocytosis and molecular sorting. Annu Rev Cell Dev Biol 1996;12:575–625. [PubMed: 8970738]

Mellman I, Fuchs R, Helenius A. Acidification of the endocytic and exocytic pathways. Annu Rev Biochem 1986;55:663–700. [PubMed: 2874766]

Mellman I, Warren G. The road taken: Past and future foundations of membrane traffic. Cell 2000;100:99–112. [PubMed: 10647935]

Merrifield CJ, Feldman ME, Wan L, Almers W. Imaging actin and dynamin recruitment during invagination of single clathrin-coated pits. Nat Cell Biol 2002;4:691–698. [PubMed: 12198492]

Merrifield CJ, Perrais D, Zenisek D. Coupling between clathrin-coated-pit invagination, cortactin recruitment, and membrane scission observed in live cells. Cell 2005;121:593–606. [PubMed: 15907472]

Morris SM, Cooper JA. Disabled-2 colocalizes with LDLR in clathrin-coated pits and interacts with AP-2. Traffic 2001;2:111–123. [PubMed: 11247302]

Motley A, Bright NA, Seaman MNJ, Robinson MS. Clathrin-mediated endocytosis in AP-2-depleted cells. J Cell Biol 2003;162:909–918. [PubMed: 12952941]

Mukherjee S, Soe TT, Maxfield FR. Endocytic sorting of lipid analogues differing solely in the chemistry of their hydrophobic tail. J Cell Biol 1999;144:1271–1284. [PubMed: 10087269]

Mundigl O, Matteoli M, Daniell L, Thomasreetz A, Metcalf A, Jahn R, de Camilli P. Synaptic vesicle proteins and early endosomes in cultured hippocampal-neurons - differential-effects of brefeldin-A in axon and dendrites. J Cell Biol 1993;122:1207–1221. [PubMed: 8376458]

Nesterov A, Carter RE, Sorkina T, Gill GN, Sorkin A. Inhibition of the receptor-binding function of clathrin adaptor protein AP-2 by dominant-negative mutant μ2 subunit and its effects on endocytosis. Embo J 1999;18:2489–2499. [PubMed: 10228163]

Nielsen E, Severin F, Backer JM, Hyman AA, Zerial M. Rab 5 regulates motility of early endosomes on microtubules. Nat Cell Biol 1999;1:376–382. [PubMed: 10559966]

Parton RG, Simons K, Dotti CG. Axonal and dendritic endocytic pathways in cultured neurons. J Cell Biol 1992;119:123–137. [PubMed: 1527164]

Pelkmans L, Burli T, Zerial M, Helenius A. Caveolin-stabilized membrane domains as multifunctional transport and sorting devices in endocytic membrane traffic. Cell 2004;118:767–780. [PubMed: 15369675]

Pelkmans L, Helenius A. Insider information: what viruses tell us about endocytosis. Curr Opin Cell Biol 2003;15:414–422. [PubMed: 12892781]

Pfeffer S, Aivazian D. Targeting RAB GTPases to distinct membrane compartments. Nat Rev Mol Cell Biol 2004;5:886–896. [PubMed: 15520808]

Rink J, Ghigo E, Kalaidzidis Y, Zerial M. Rab conversion as a mechanism of progression from early to late endosome. Cell 2005;122:735–749. [PubMed: 16143105]

Robinson MS. Adaptable adaptors for coated vesicles. Trends Cell Biol 2004;14:167–174. [PubMed: 15066634]

Rust MJ, Lakadamyali M, Zhang F, Zhuang X. Assembly of endocytic machinery around individual influenza viruses during viral entry. Nat Struct Mol Biol 2004;11:567–573. [PubMed: 15122347]

Schmid SL. Clathrin-coated vesicle formation and protein sorting. Annu Rev Biochem 1997;66:511–548. [PubMed: 9242916]

Sheff D, Pelletier L, O'Connell CB, Warren G, Mellman I. Transferrin receptor recycling in the absence of perinuclear recycling endosomes. J Cell Biol 2002;156:797–804. [PubMed: 11877458]

Sheff DR, Daro EA, Hull M, Mellman I. The receptor recycling pathways contains two distinct populations of early endosomes with different sorting function. J Cell Biol 1999;145:123–139. [PubMed: 10189373]

Sieczkarski SB, Whittaker GR. Influenza virus can enter and infect cells in the absence of clathrin-mediated endocytosis. J Virol 2002;76:10455–10464. [PubMed: 12239322]

Sigismund S, Woelk T, Puri C, Maspero E, Tacchetti C, Transidico P, Di Fiore PP, Polo S. Clathrin-independent endocytosis of ubiquitinated cargos. Proc Natl Acad Sci, USA 2005;102:2760–2765. [PubMed: 15701692]

Sonnichsen B, De Renzis S, Nielsen E, Rietdorf J, Zerial M. Distinct membrane domains on endosomes in the recycling pathway visualized by multicolor imaging of Rab4, Rab5 and Rab11. J Cell Biol 2000;149:901–913. [PubMed: 10811830]

Sorkin A. Cargo recognition during clathrin-mediated endocytosis: a team effort. Curr Opin Cell Biol 2004;16:392–399. [PubMed: 15261671]

Stoorvogel W, Strous GJ, Geuze HJ, Oorschot V, Schwartz AL. Late endosomes derive from early endosomes by maturation. Cell 1991;65:417–427. [PubMed: 1850321]

Tanowitz M, von Zastrow M. A novel endocytic recycling signal that distinguishes the membrane trafficking of naturally occurring opioid receptors. J Biol Chem 2003;278:45978–45986. [PubMed: 12939277]

Traub LM. Sorting it out: AP-2 and alternate clathrin adaptors in endocytic cargo selection. J Cell Biol 2003;163:203–208. [PubMed: 14581447]

Trowbridge IS, Collawn JF, Hopkins CR. Signal dependent membrane protein trafficking in the endocytic pathway. Annu Rev Cell Biol 1993;9:129–161. [PubMed: 8280459]

Ullrich O, Reinsch S, Urbe S, Zerial M, Parton RG. Rab11 regulates recycling through pericentriolar recycling endosomes. J Cell Biol 1996;135:913–924. [PubMed: 8922376]

van Leuven F, Cassiman JJ, van den Berghe H. Primary amines inhibit recycling of alpha-2m receptors in fibroblasts. Cell 1980;20:37–43. [PubMed: 6156003]

Vonderheit A, Helenius A. Rab7 associates with early endosomes to mediate sorting and transport of semliki forest virus to late endosomes. PLOS Biol 2005;3:1225–1238.

Wall DA, Wilson G, Hubbard AL. The galactose-specific recognition system of mammalian liver - the route of ligand internalization in rat hepatocytes. Cell 1980;21:79–93. [PubMed: 7407914]

Watanabe R, Asakura K, Rodriguez M, Pagano RE. Internalization and sorting of plasma membrane sphingolipid analogues in differentiating oligodendrocytes. J Neurochem 1999;73:1375–1383. [PubMed: 10501180]

Wei ML, Bonzelius F, Scully R, Kelly RB, Herman GA. GLUT4 and transferrin receptor are differentially sorted along the endocytic pathway in CHO cells. J Cell Biol 1998;140:565–575. [PubMed: 9456317]

Yamashiro DJ, Maxfield FR. Acidification of morphologically distinct endosomes in mutant and wild-type chinese-hamster ovary cells. J Cell Biol 1987;105:2723–2733. [PubMed: 2447098]

Yishimura A, Ohnishi S. Uncoating of influenza virus in endosomes. J Virol 1984;51:497–504. [PubMed: 6431119]

Zerial M, McBride H. Rab proteins as membrane organizers. Mol Cell Biol 2001;2:107–119.

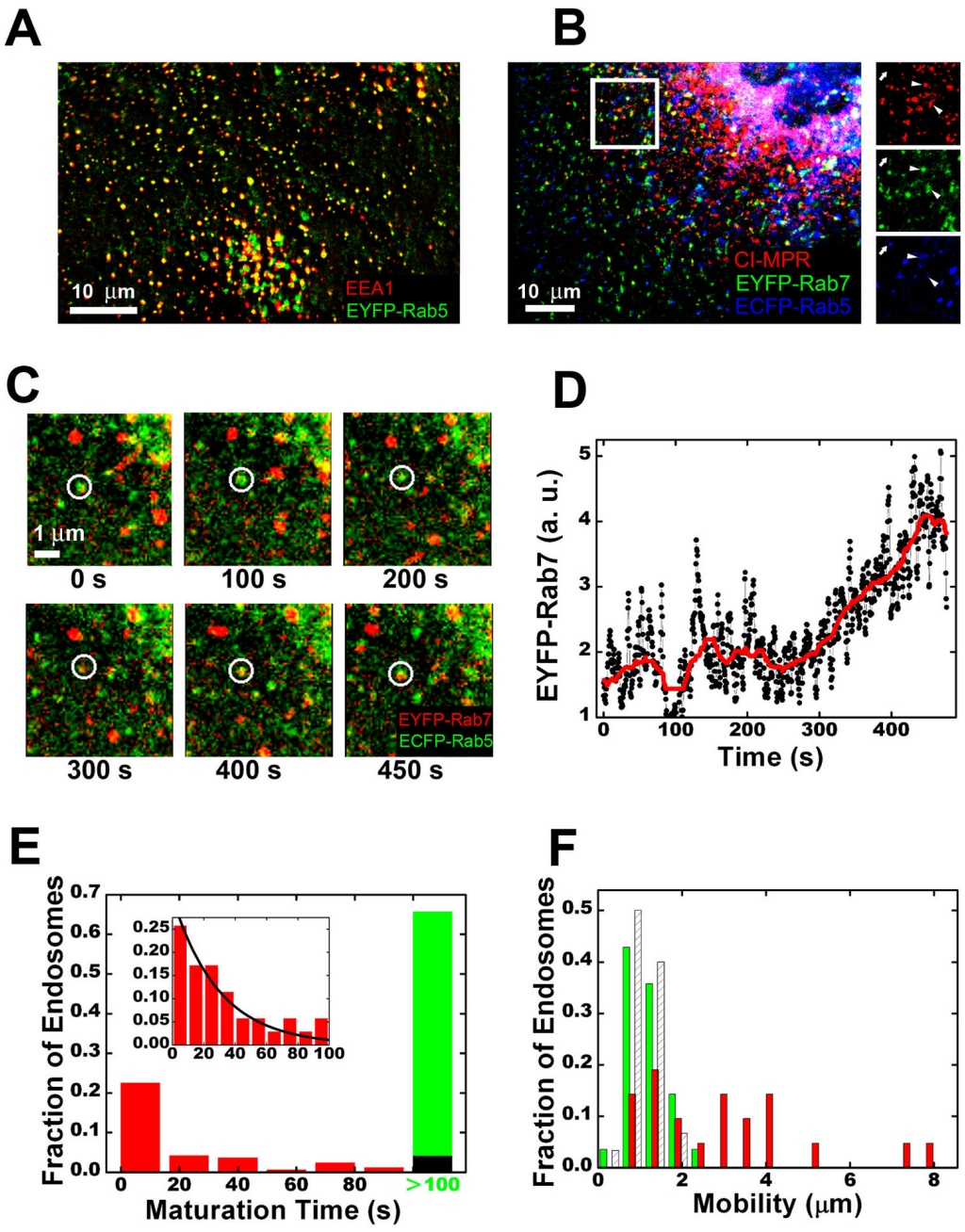

Figure 1.

Early endosomes are comprised of two populations with distinct maturation kinetics and mobility. (A) Colocalization between Rab5 and EEA1. EEA1 was detected by immunofluorescence; Rab5 was detected by EYFP-Rab5. (B) Colocalization between Rab5, Rab7 and CI-MPR. CI-MPR was detected by immunofluorescence; Rab5 and Rab7 were detected by ECFP-Rab5 and EYFP-Rab7, respectively. The boxed region is magnified and shown in separated channels on the right. Arrowheads mark CI-MPR-positive spots that also contain Rab5 and Rab7; the arrow marks a Rab5-only endosome without CI-MPR. (C) The maturation of a Rab5-positive endosome as shown by the accumulation of Rab7 (see Movie S2). (D) The raw (black) and median-filtered (red) time-dependence of the EYFP-Rab7

intensity associated with the endosome shown in (C). (E) A histogram of the maturation time of many randomly selected Rab5-positive endosomes. Image acquisition begins at time = 0 and the maturation time is operationally defined as the time when the endosome accumulates detectable amount of Rab7. The green bar indicates endosomes with maturation time > 100 s. About 14% of the Rab5-positive endosomes already contain Rab7 at time = 0, these endosomes are included in the first bin. The inset is the maturation time histogram for the endosomes starting with only Rab5 and acquiring Rab7 within 100 seconds. The fit to a single exponential (black line) yields a time constant of 30 s. The black bar in the main histogram is the expected fraction of endosomes with maturation time > 100 s if all endosomes matured with the same single-exponential kinetics. (F) A mobility histogram of randomly selected Rab5-positive endosomes. The mobility is defined as the diameter of the smallest circle enclosing the trajectory of the endosome in 100 s. The slowly maturing endosomes (maturation time > 100 s, green) are relatively stationary compared to the rapidly maturing endosomes (maturation time ≤ 100 s, red). The shaded columns show a mobility histogram of all early endosomes in nocodazole-treated cells.

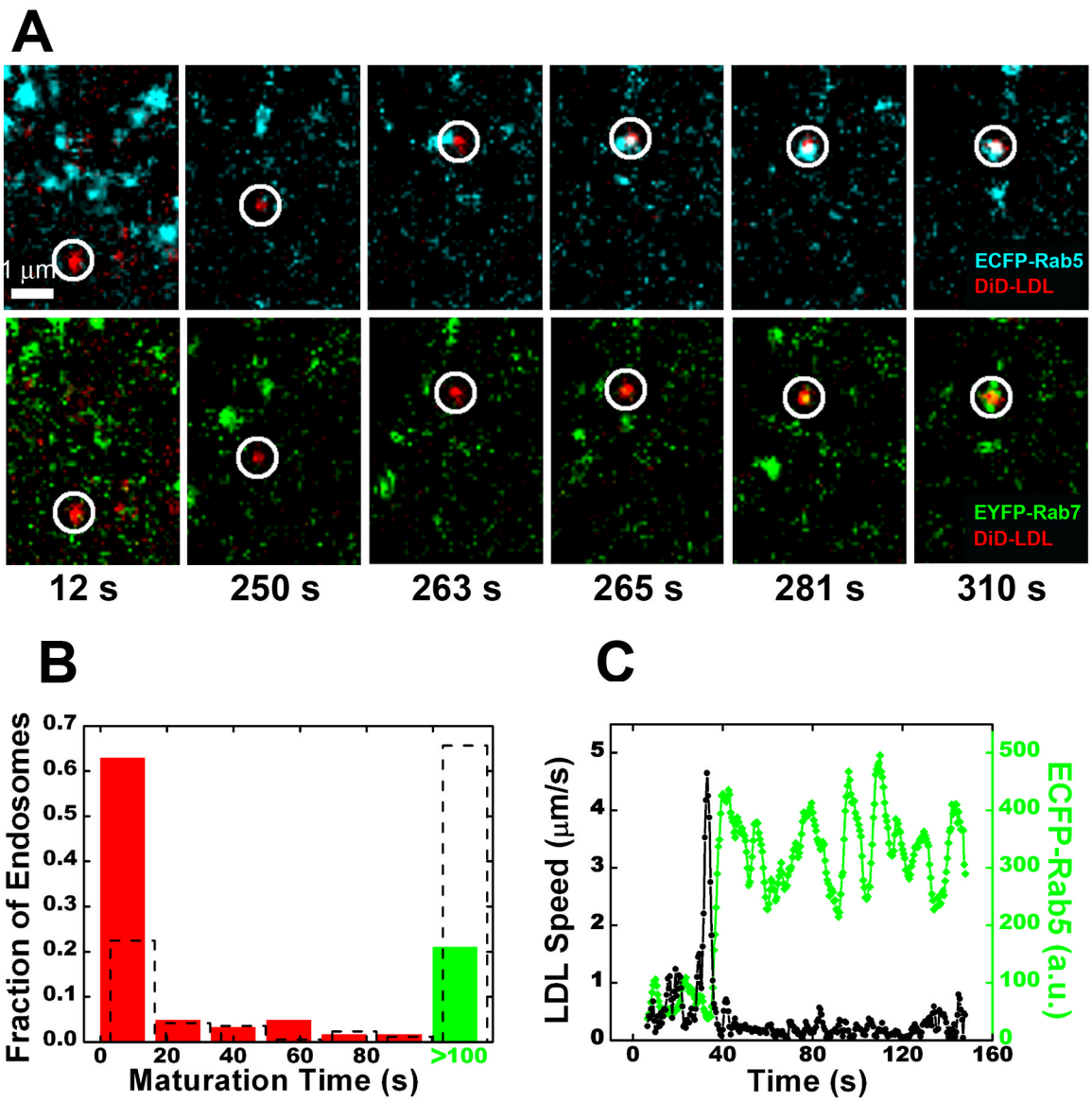

Figure 2.

LDL is predominantly targeted to the dynamic population of early endosomes directly. (A) Selected frames from an LDL particle being trafficked to a rapidly maturing endosome (see Movie S4). The temperature was raised from 0 to 37 °C at time = 0. (B) A histogram of maturation times for endosomes receiving LDL. Overlaid is the histogram of all Rab5-positive endosomes (dashed columns). (C) Time trajectories of the velocity (black) of an LDL particle and the ECFP-Rab5 signal (green) associated with that particle. The large velocity spike indicates a long-range microtubule-dependent movement toward the perinuclear region, typically observed for endocytic ligands bound for degradation. These velocity spikes are abolished in cells treated with nocodazole.

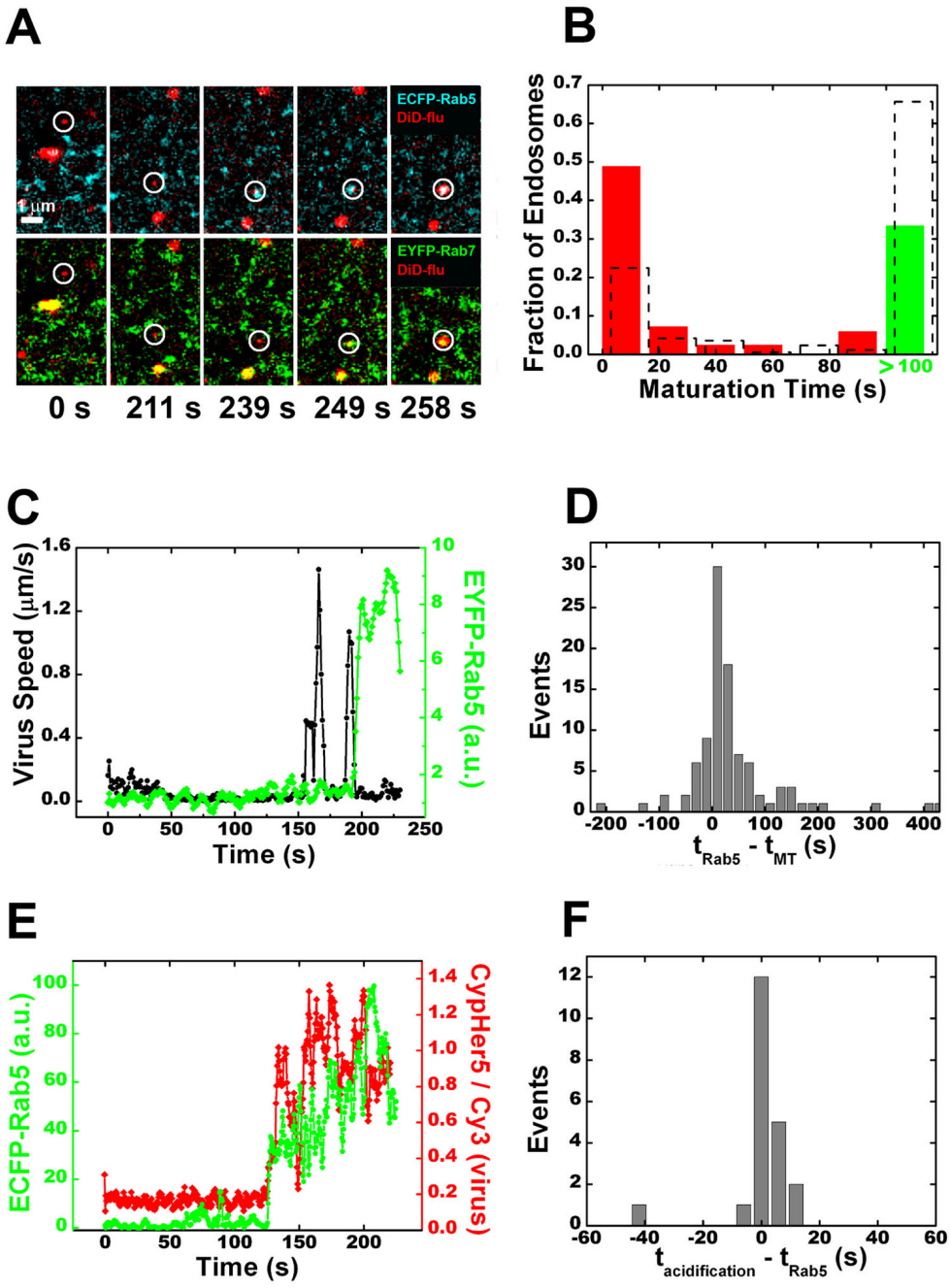

Figure 3.

Influenza viruses are preferentially sorted to the dynamic population of early endosomes. (A) Selected frames from a virus particle being trafficked to a rapidly maturing endosome and subsequent fusion with that endosome (see Movie S5). Fusion is indicated by a sudden increase in DiD signal due to fluorescence dequenching. Virus particles were added to the cell culture *in situ* and time = 0 is set for each virus when it binds to the cell. (B) A histogram of maturation times for endosomes receiving influenza. Overlaid is the histogram for all Rab5-positive endosomes (dashed columns). (C) Time trajectories of the velocity (black) of a virus particle and the Rab5 signal (green) associated with the virus. The large velocity spikes indicate long-range microtubule-dependent motion. (D) A histogram of the time lag between virus particles

entering a Rab5-positive endosome (t_{Rab5}) and the onset of microtubule-dependent movement (t_{MT}). (E) Time trajectories of the environmental acidity (red) experienced by a virus particle and the ECFP-Rab5 intensity (green) associated with the virus particle. Acidification is measured as a change in the intensity ratio between CypHer5 (a pH-sensitive dye) and Cy3 (a pH-independent dye) attached to the virus. Calibration shows that the CypHer5/Cy3 ratio changes most significantly when pH changes from neutral to pH 6 (Lakadamyali et al., 2003). (F) A histogram of the time lag between viruses joining a Rab5-positive endosome (t_{Rab5}) and the initial acidification of the virus particle ($t_{acidification}$).

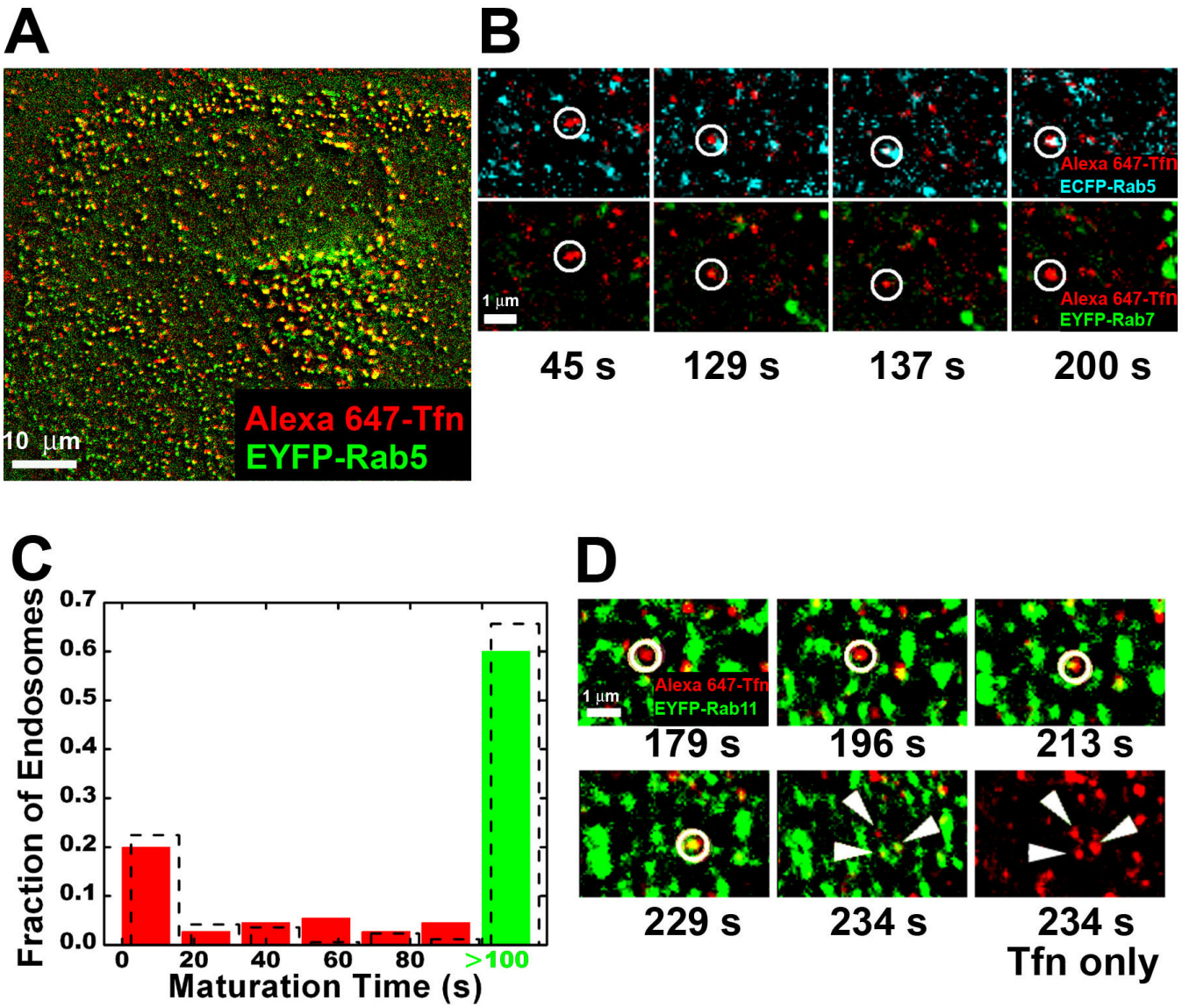

Figure 4.

Transferrin is non-selectively delivered to all early endosomes. (A) Colocalization between transferrin (Tfn) and Rab5 in a cell after 5 minutes of transferrin uptake. (B) Selected frames showing a transferrin-containing vesicle being delivered to a Rab5-positive endosome that does not accumulate Rab7 within 100 s. The temperature of the sample was raised from 0 to 37 °C at time = 0. (C) The maturation time histogram of the endosomes receiving transferrin. The histogram for all endosomes (dashed columns) is overlaid for comparison. (D) Association of transferrin with Rab11-labeled recycling endosome and the subsequent tubulation and fission of the transferrin spot into several spots (arrowheads) (see Movies S6A,B).

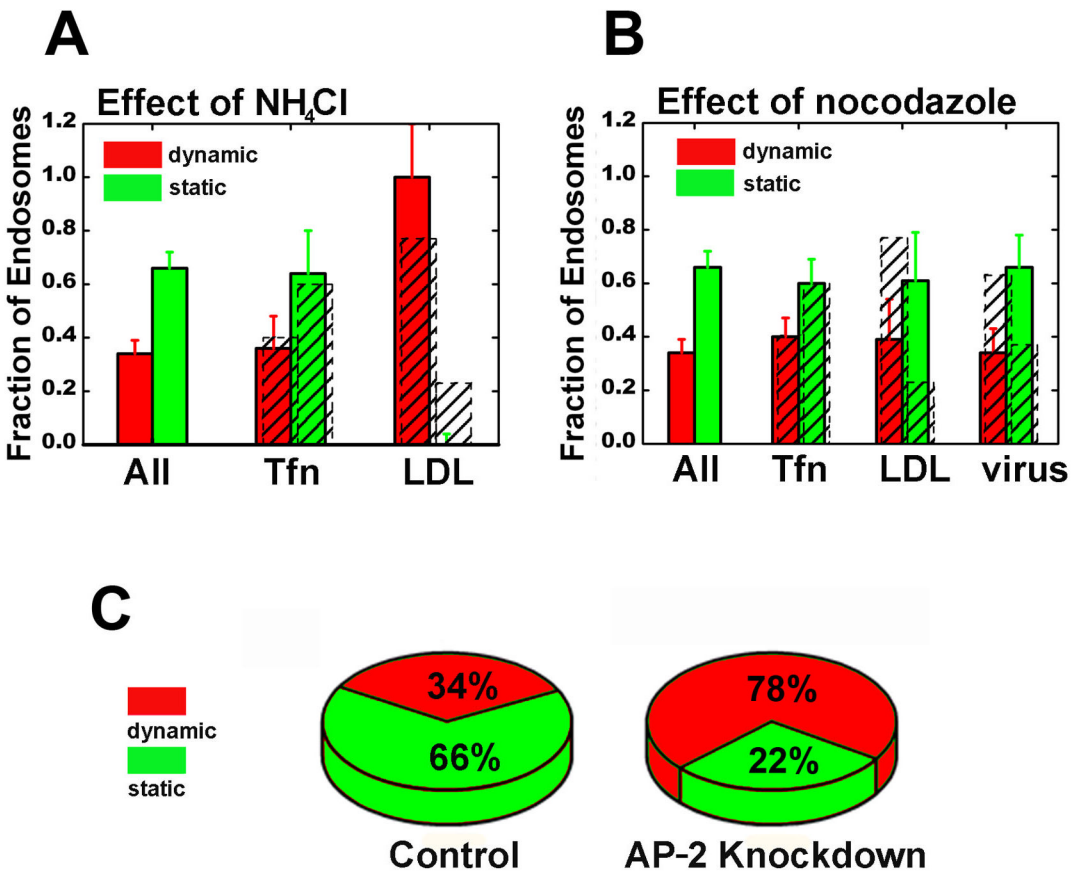

Figure 5.

The pre-early endosome sorting is independent of pH, but depends on microtubules and endocytic adaptor protein. (A) The effect of ammonium chloride on the balance between the dynamic (maturation time < 100 s) and static (maturation time > 100 s) endosome populations. (B) The effect of nocodazole (30 min treatment) on the balance between the two populations. In (A) and (B), colored histograms are for all endosomes, Tfn-receiving, LDL-receiving, and virus-receiving endosomes in drug-treated cells; shaded histograms are for those in untreated cells. (C) The effect of AP-2 knockdown on the balance between the two populations.

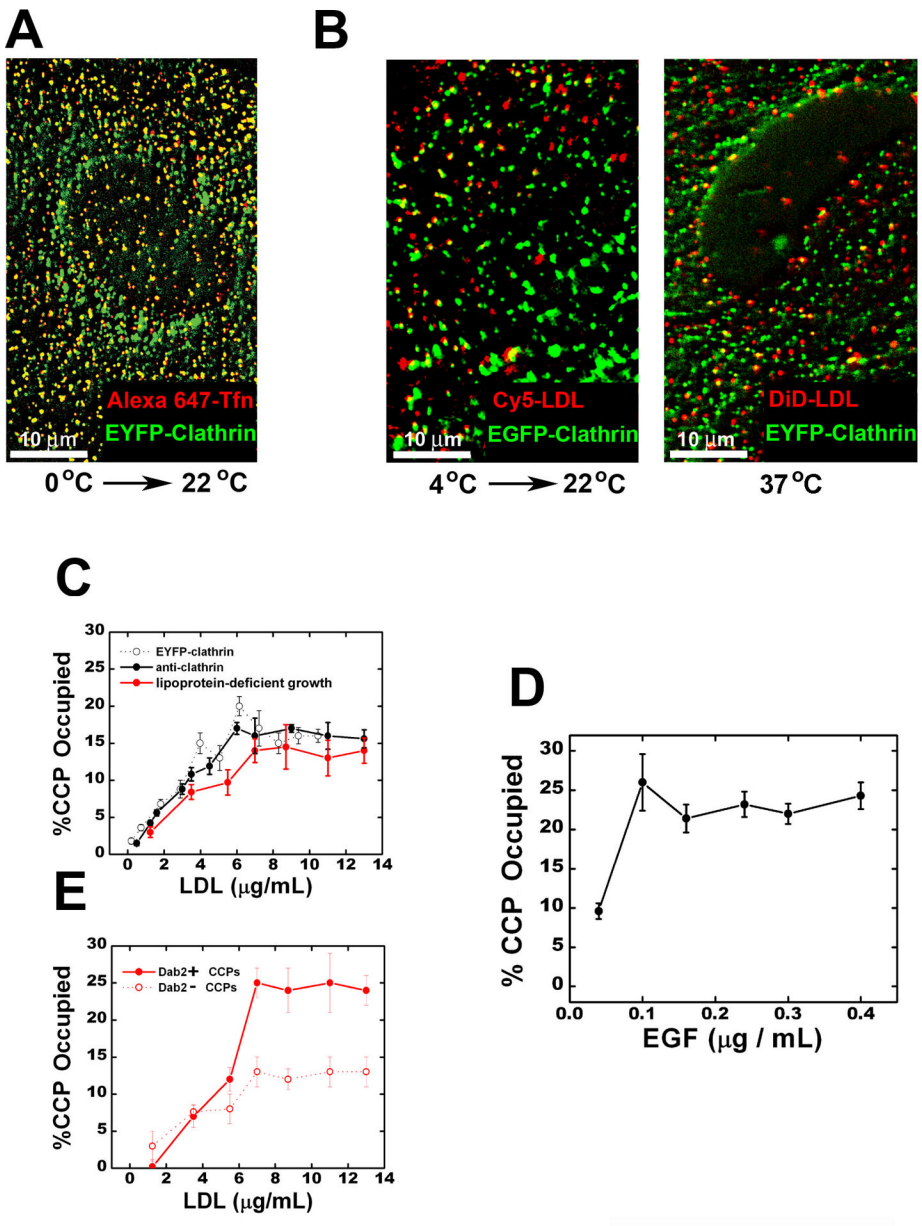

Figure 6.

Enrichment of LDL and EGF in a subset of clathrin-coated pits (CCPs). (A) Colocalization between transferrin and clathrin. Transferrin was bound to EYFP-clathrin expressing cells at 0°C for 10 min and then imaged immediately at room temperature. (B) Colocalization between LDL and clathrin. Left panel: LDL (10 μg/ml) was bound to EYFP-clathrin expressing cells at 4°C for 10 min and then imaged immediately at room temperature. Right panel: LDL was incubated with EYFP-clathrin expressing cells at 37°C for 3 min before fixation and imaging. (C) The fraction of CCPs containing LDL as a function of the LDL concentration used. Here, LDL was incubated with cells at 37°C for 3 min. Longer LDL incubation time did not change the results. The fraction determined in EYFP-clathrin expressing cells is shown in open black symbols. To assess the effect of EYFP-clathrin expression, we determined the fraction of CCPs containing LDL in cells not expressing EYFP-clathrin (solid black symbols), with clathrin detected by immunofluorescence. Red symbols indicated results obtained in cells incubated

with lipoprotein-deficient serum overnight to up-regulate LDLR expression (red symbols). (D) The fraction of CCPs containing EGF as a function of EGF concentration. The experiments were carried out similarly to (C). (E) Role of Dab2. After incubation of EGFP-clathrin expressing cells with LDL for 3 min at 37°C, cells were saponin-extracted, fixed and immunostained for Dab2. CCPs show significant colocalization with Dab2 and the quantitative extent of colocalization is cell-type dependent (Figure S6A). Solid and open red symbols, respectively, indicate the fraction of Dab2-positive and Dab2-negative CCPs containing LDL. The cells were incubated with lipoprotein-deficient serum overnight.

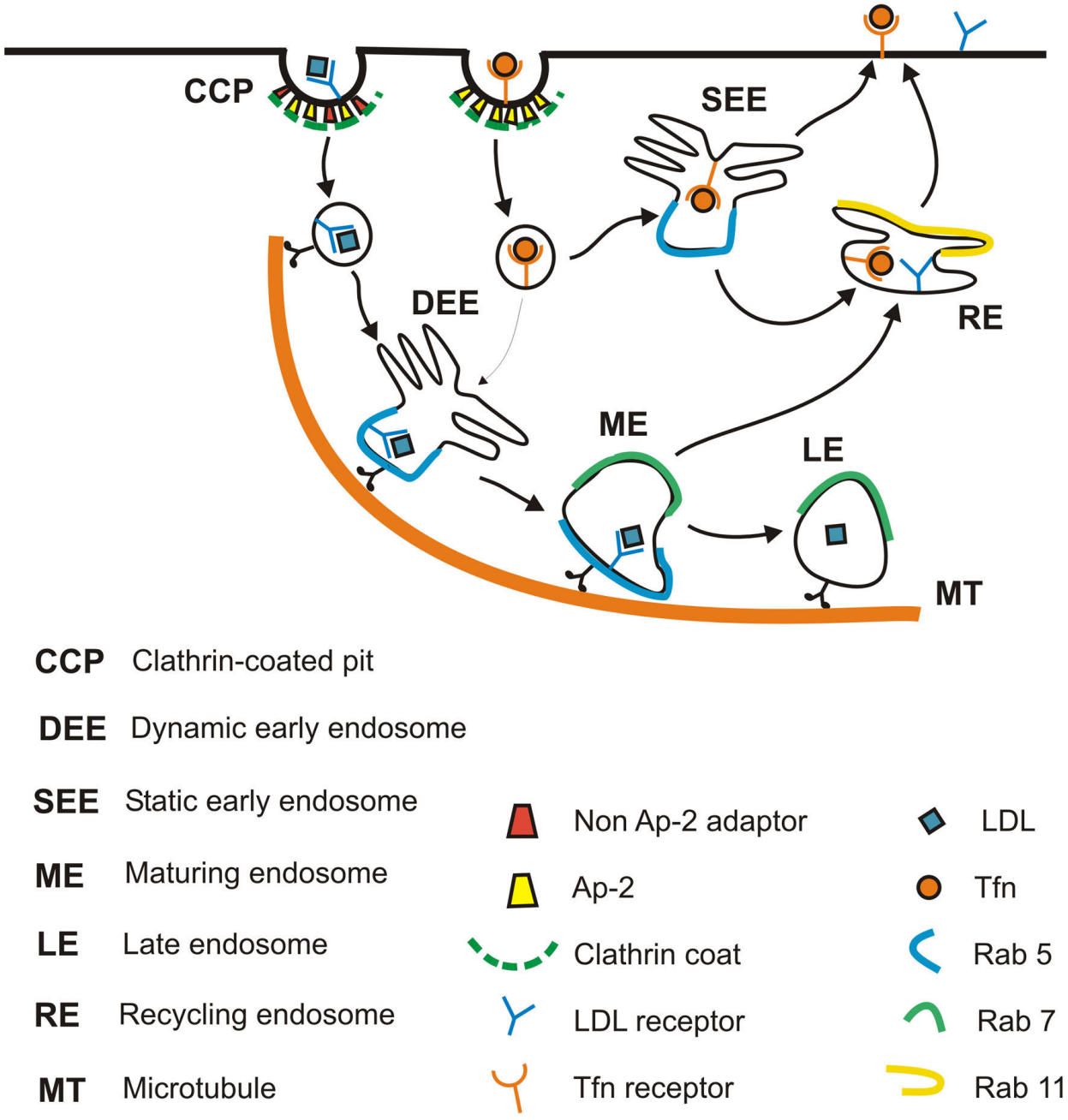

Figure 7.

A proposed model for pre-early endosome sorting that differentially targets endocytic cargos into distinct populations of coated vesicles and early endosomes. Early endosomes are comprised of a dynamic population that matures quickly towards late endosomes and a relatively static population that matures much more slowly. Several cargos destined for degradation, including LDL, EGF and influenza virus, are internalized by a subpopulation(s) of clathrin-coated vesicles, which likely contain alternative adaptors in addition to AP-2. These vesicles rapidly engage microtubules and are consequently targeted to the dynamic population of early endosomes, which are also moving on microtubules. The recycling ligand transferrin is indiscriminately recruited to all clathrin-coated vesicles and thus delivered to both

populations of early endosomes non-selectively, effectively being enriched in the larger, static population.